Journal of Sound and Vibration (1999) **220**(4), 577–599
Article No. jsvi.1998.1927, available online at http://www.idealibrary.com on IDEAL

THREE-DIMENSIONAL VIBRATION ANALYSIS OF RECTANGULAR PLATES BASED ON DIFFERENTIAL QUADRATURE METHOD

K. M. Liew and T. M. Teo

Centre for Advanced Numerical Engineering Simulations, *School of Mechanical and Production Engineering*, *Nanyang Technological University*, *Nanyang Avenue*, *Singapore* 639798

(*Received* 10 *February* 1997, *and in final form* 30 *July* 1998)

This paper presents the formulation and numerical analysis of the three-dimensional elasticity plate model using the differential quadrature (DQ) method. The governing equations in terms of displacement, stress–displacement relations, and boundary conditions for the three-dimensional plate model are first presented. These equations are then normalized and discretized using the DQ procedure. Example problems on the free vibration of rectangular plates with generic boundary conditions are selected. Two types of mesh pattern, the uniform mesh pattern and the cosine mesh pattern, were used and their convergence characteristics were studied. The cosine mesh was then chosen as the better mesh pattern pertaining to the problems solved. The solutions calculated using the cosine mesh pattern were then compared, where possible, with the exact or the numerical or the analytical solutions. It is found that the differential quadrature method yields accurate results for the plate problems under the current investigation.

1. INTRODUCTION

In the field of sciences and engineering, the solutions to practical problems are usually described by simultaneous partial differential equations. It is commonly agreed that exact or analytical solutions to such equations are both difficult and tedious. Such solutions are even more difficult as the order of the partial differential equations becomes higher and the number of independent variables becomes greater. This gives rise to the popularity of numerical methods in solving such equations.

Currently, conventional numerical methods like low order finite differences and finite element methods are used for such problems. These methods usually need a large number of grid points in order to arrive at the convergent and accurate solution. This large number of grid points is sometimes redundant and wastes computational resources if the problem needs only a small number of grid points. An example of such is in the calculation of the maximum deflection of a uniformly loaded structure. Obviously, the location where the maximum deflection occurs can be easily predicted. Also, in the solution of global problems like buckling or

0022–460X/99/090577 + 23 $30.00/0

free vibration analysis, the number of grid points used is immaterial. Much research was thus conducted to develop numerical methods that address such needs. The differential quadrature (DQ) method is one of them.

The DQ method was proposed by the late Richard Bellman and his associates [1–3]. It was reported that this method was able to rapidly compute accurate solution of partial differential equations by using only a few grid points in the respective solution domain [4]. In short, this DQ method approximates the partial derivatives of a function with respect to spatial discrete points using the weighted linear sum of the function values at all the discrete points in the overall domain of the spatial variable [2, 5–7]. This method is able to reduce the set of partial differential equation to a set of algebraic equations for time independent problems and a set of ordinary differential equations for time dependent problems.

There are basically four approaches in calculating the weighting coefficients of the DQ approximation. The first is the power polynomials approach, proposed by Bellman [2]. Unfortunately, the system of equations to be solved using this approach becomes ill conditioned when the number of grid points chosen is too large. The second is the use of the roots of the shifted Legendre polynomials as the test function which subsequently is used to calculate the weighting coefficient. The limitation of this method is it restricts the type of mesh pattern used. This imposes a major drawback in structural analysis as all sorts of boundary conditions could appear and different mesh grids may be needed for different boundary conditions. The third approach was proposed by Quan and Chang [7]. It uses the Jacobi orthogonal polynomials as the test function. As the Legendre polynomials belong to the family of Jacobi orthogonal polynomials, this approach faces the same limitations as the second approach. The fourth approach, also proposed by Quan and Chang [7], adopts the Lagrange interpolated polynomials as the test function instead of the power polynomials or Legendre polynomials. In the paper, Quan and Chang derived the first and second order weighting coefficients. Followed [7], Shu and Richard [8] used the same test function and derived the higher order weighing coefficients in the form of a recurrence relationship. The method proposed by Shu and Richard [8] shall be used for the calculation of the weighting coefficients in this paper.

The pioneer work for application of DQ method to structural mechanics was carried out by Bert *et al*. [4, 9, 10], Wang and Bert [11] and Wang *et al*. [12, 13]. Other researchers in this area include Liu and Liew [14, 15], Du *et al*. [16], Laura and Gutierrez [17], Wen and Yu [18], Han and Liew [19, 20], Liew *et al*. [21, 22] and Liew and Han [23, 24]. In the area on three-dimensional plate analysis, Teo and Liew [25, 26], Liew and Teo [27] and Teo [28] researched into the DQ application pertaining to bending, buckling and free vibration of isotropic and orthotropic plates. In 1998, Malik and Bert [29]† employed the DQ method to solve free vibration three-dimensional elastic thick plates that have at least one pair of opposite edges simply-supported.

Numerous methods have been proposed by earlier researchers for solving plate problems based on three-dimensional elasticity theory [30–38]. These

† This reference was brought to the authors' attention by one of the reviewers.

three-dimensional solutions are extremely useful in evaluating the accuracy of approximate results, for instance, in the case of two-dimensional plate theories. In this paper, we employ the DQ method for three-dimensional free vibration analysis of rectangular plates having generic boundary conditions.

This paper is organized as follows. In section 2, the DQ procedures are briefly described. In section 3, the three-dimensional equilibrium equations and the boundary conditions are outlined. In section 4, the details of the normalization and discretization of the three-dimensional linear elasticity equations and boundary conditions are presented. In section 5, the ease of use, and the convergence characteristics and accuracy of the DQ method are demonstrated through the solving of numerical test examples for which exact solutions or numerical solutions are available for comparison. Finally, the conclusions from this study are drawn in section 6.

2. DIFFERENTIAL QUADRATURE METHOD

We first consider a function $f(x)$ in one-dimensional space. The DQ method approximates the first derivative of this function at the ith discrete point on a grid by

$$f'(x_i) = \sum_{l=1}^{N} A_{il}^{(1)} f(x_1) \qquad \text{for } i = 1, 2, 3, \ldots, N \tag{1}$$

where N is the total number of grid points chosen for the solution domain in the x direction and $A_{il}^{(n)}$ is the weighting coefficient of the ith point approximation of the function $f(x)$. The superscript n represents the nth derivative of the function.

The weighing coefficients $A_{il}^{(n)}$ can be obtained using the following recurrence formulas:

$$A_{il}^{(1)} = \frac{M^{(1)}(x_i)}{(x_i - x_1)M^{(1)}(x_1)} \qquad \text{for } i \neq 1; \quad i, l = 1, 2, 3, \ldots, N \tag{2a}$$

$$A_{il}^{(n)} = n\left(A_{il}^{(n-1)} A_{ll}^{(n)} - \frac{A_{il}^{(n-1)}}{x_i - x_1}\right) \qquad \text{for } i \neq 1;$$

$$n = 2, 3, \ldots, N-1; \quad i, l = 1, 2, 3, \ldots, N \tag{2b}$$

and

$$A_{ii}^{(n)} = -\sum_{l=1, l=i}^{N} A_{il}^{(n)} \qquad \text{for } i = 1, 2, 3, \ldots, N. \tag{2c}$$

For equation (2a), $M^{(1)}$ is denoted by the following expression:

$$M^{(1)}(x_p) = \prod_{l=1, l\neq k}^{N} (x_p - x_1). \tag{3}$$

An elaborated presentation of the DQ method can be obtained from the work by Du *et al*. [14] and the excellent review by Bert and Malik [39].

The above DQ approximation is shown for a one-dimensional case. The three-dimensional DQ approximation can be easily extended from the above. The DQ method approximates the function $f(x, y, z)$ as required in the three-dimensional formulation of this paper and is detailed as follows.

The first-order derivatives can be approximated by

$$\left.\frac{\partial f}{\partial x}\right|_{ijk} \approx \sum_{l=1}^{N_x} A_{il}^{(1)} f_{ljk}; \qquad \left.\frac{\partial f}{\partial y}\right|_{ijk} \approx \sum_{m=1}^{N_y} B_{jm}^{(1)} f_{imk}; \qquad \left.\frac{\partial f}{\partial z}\right|_{ijk} \approx \sum_{n=1}^{N_z} C_{kn}^{(1)} f_{ijn}. \quad (4a\text{–}c)$$

The second-order derivatives can be approximated by

$$\left.\frac{\partial^2 f}{\partial x^2}\right|_{ijk} \approx \sum_{l=1}^{N_x} A_{il}^{(2)} f_{ljk}; \qquad \left.\frac{\partial^2 f}{\partial y^2}\right|_{ijk} \approx \sum_{m=1}^{N_y} B_{jm}^{(2)} f_{imk}; \qquad \left.\frac{\partial^2 f}{\partial z^2}\right|_{ijk} \approx \sum_{n=1}^{N_z} C_{kn}^{(2)} f_{ijn} \quad (5a\text{–}c)$$

$$\left.\frac{\partial}{\partial x}\left(\frac{\partial f}{\partial y}\right)\right|_{ijk} \approx \sum_{l=1}^{N_x} A_{il}^{(1)} \sum_{m=1}^{N_y} B_{jm}^{(1)} f_{lmk}; \qquad \left.\frac{\partial}{\partial x}\left(\frac{\partial f}{\partial z}\right)\right|_{ijk} \approx \sum_{l=1}^{N_x} A_{il}^{(1)} \sum_{n=1}^{N_z} C_{kn}^{(1)} f_{ljn}; \quad (6a, b)$$

$$\left.\frac{\partial}{\partial y}\left(\frac{\partial f}{\partial z}\right)\right|_{ijk} \approx \sum_{m=1}^{N_y} B_{jm}^{(1)} \sum_{n=1}^{N_z} C_{kn}^{(1)} f_{imn} \quad (6c)$$

where A, B and C denote the weighting coefficients of the partial derivative of the function $f(x, y, z)$ with respect to the x, y and z directions respectively; N_x, N_y and N_z are the number of grid points chosen in the x, y and z directions respectively.

3. BASIC GOVERNING EQUATIONS

3.1. EQUILIBRIUM EQUATIONS

The equations of motion in terms of displacement for a homogeneous isotropic plate without body force can be written as:

$$\nabla^2 u + \frac{1}{1-2v}\frac{\partial e}{\partial x} + \frac{\rho\omega^2 u}{G} = 0 \quad (7a)$$

$$\nabla^2 v + \frac{1}{1-2v}\frac{\partial e}{\partial y} + \frac{\rho\omega^2 v}{G} = 0 \quad (7b)$$

$$\nabla^2 w + \frac{1}{1-2v}\frac{\partial e}{\partial z} + \frac{\rho\omega^2 w}{G} = 0 \quad (7c)$$

where ρ is the density, e is the dilatation defined by

$$e = (\partial/\partial x; \partial/\partial y; \partial/\partial z)\{u, v, w\}^{\mathrm{T}} \quad (7d)$$

and

$$\nabla^2 = \frac{\partial^2}{\partial x^2} + \frac{\partial^2}{\partial y^2} + \frac{\partial^2}{\partial z^2}. \quad (7e)$$

The variables u, v and w are the displacements in the x, y and z-directions as depicted in the co-ordinate system respectively. This co-ordinate system is shown in Figure 1. The symbols v and ω represent the Poisson ratio and the angular frequency of the plate respectively. In this paper, E and G are the Young's and shear moduli of the plate respectively.

The stress–displacement relation are given as:

$$\begin{bmatrix} \sigma_x \\ \sigma_y \\ \sigma_z \\ \tau_{xy} \\ \tau_{xz} \\ \tau_{yz} \end{bmatrix} = \begin{bmatrix} \varphi(1-v)\dfrac{\partial}{\partial x} & \varphi v \dfrac{\partial}{\partial y} & \varphi v \dfrac{\partial}{\partial z} \\ \varphi v \dfrac{\partial}{\partial x} & \varphi(1-v)\dfrac{\partial}{\partial y} & \varphi v \dfrac{\partial}{\partial z} \\ \varphi v \dfrac{\partial}{\partial x} & \varphi v \dfrac{\partial}{\partial y} & \varphi(1-v)\dfrac{\partial}{\partial z} \\ G\dfrac{\partial}{\partial y} & G\dfrac{\partial}{\partial x} & 0 \\ G\dfrac{\partial}{\partial z} & 0 & G\dfrac{\partial}{\partial x} \\ 0 & G\dfrac{\partial}{\partial z} & G\dfrac{\partial}{\partial y} \end{bmatrix} \times \begin{bmatrix} u \\ v \\ w \end{bmatrix} \tag{8}$$

where φ is defined as $\varphi = 2G/(1-2v)$.

In the above equations σ_x, σ_y and σ_z represent the stresses in the x, y and z-directions respectively; τ_{xy}, τ_{xz} and τ_{yx} are the shear stresses.

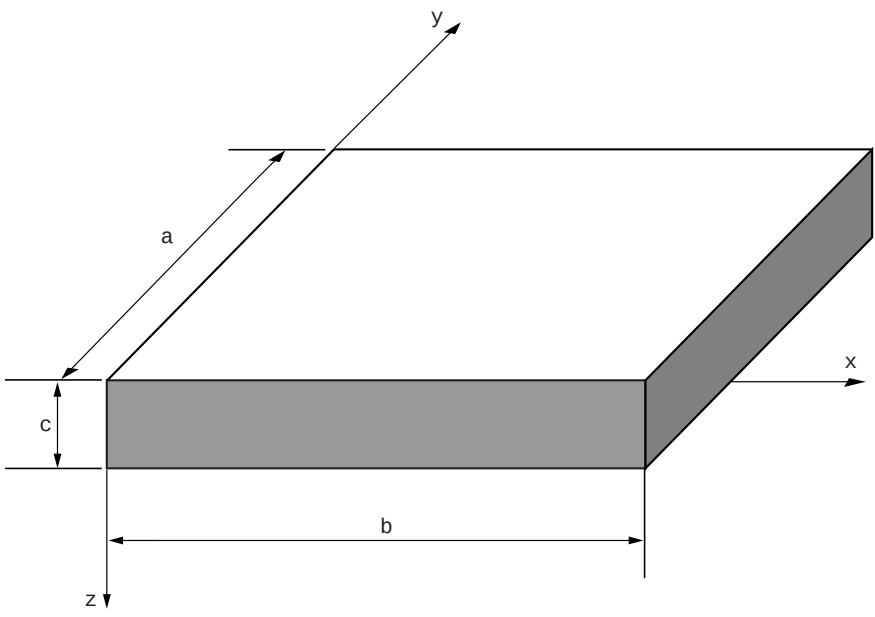

Figure 1. Co-ordinate system and dimensions.

3.2. BOUNDARY CONDITIONS

In three-dimensional numerical analysis of a plate, the boundary conditions need to apply to all six faces of the solid. The four faces where $x = 0$, a and $y = 0$, b are called the edge boundary conditions whereas the top and bottom surfaces of the plate are called the surface boundary condition.

In this paper, the free surface boundary condition shall be used in the discussion. Also, two types of edge boundary conditions are considered. They are namely the fully clamped boundary condition (C) and the simply supported boundary conditions (S). Following are the equations describing the boundary conditions:

- Clamped boundary condition (C)

$$u = 0; \qquad v = 0; \qquad w = 0. \tag{9}$$

- Hard simply supported boundary condition (S)

$$\text{On } x = 0 \text{ and } a: \qquad \sigma_x = 0; \qquad v = 0; \qquad w = 0 \tag{10a}$$

$$\text{On } y = 0 \text{ and } b: \qquad \sigma_y = 0; \qquad u = 0; \qquad w = 0. \tag{10b}$$

- Free surface condition

$$\text{On } z = 0, c: \qquad \sigma_z = 0; \qquad \tau_{xz} = 0; \qquad \tau_{yz} = 0. \tag{11}$$

4. METHOD OF SOLUTION

4.1. GOVERNING EQUATIONS

In order to normalize the above equations, the following non-dimensional parameters are introduced.

$$X = \frac{x}{a}; \qquad Y = \frac{y}{b}; \qquad Z = \frac{z}{c}; \tag{12a–c}$$

$$U = \frac{u}{a}; \qquad V = \frac{v}{b}; \qquad W = \frac{w}{a}; \tag{12d–f}$$

$$\alpha = \frac{a}{b}; \qquad \beta = \frac{c}{b}; \qquad \gamma = \frac{c}{a} \tag{12g–i}$$

$$\tau_{XY} = \frac{\tau_{xy}}{G}; \qquad \tau_{XZ} = \frac{\tau_{xz}}{G}; \qquad \tau_{YZ} = \frac{\tau_{yz}}{G} \tag{12j–l}$$

$$\sigma_X = \frac{\gamma(1-2\nu)\sigma_x}{2G}; \qquad \sigma_Y = \frac{\gamma(1-2\nu)\sigma_y}{2G}; \qquad \sigma_Z = \frac{\gamma(1-2\nu)\sigma_z}{2G}. \tag{12m–0}$$

In the above equations, a, b and c represent the lengths in the x, y and z-directions of the plate respectively.

4.2. NORMALIZATION AND DISCRETIZATION OF THE EQUILIBRIUM EQUATIONS

Substituting equations (12) into the equilibrium equations [equations (7)] results in the following normalized governing equations

$$2\gamma^2(1-\nu)\frac{\partial^2 U}{\partial X^2}+\beta^2(1-2\nu)\frac{\partial^2 U}{\partial Y^2}+(1-2\nu)\frac{\partial^2 U}{\partial Z^2}+\gamma^2\frac{\partial^2 V}{\partial X\,\partial Y}+\gamma\frac{\partial^2 W}{\partial X\,\partial Z}$$
$$=2c^2(1+\nu)(2\nu-1)\frac{\rho\omega^2}{E}U \tag{13a}$$

$$\beta^2\frac{\partial^2 U}{\partial X\,\partial Y}+\gamma^2(1-2\nu)\frac{\partial^2 V}{\partial X^2}+2\beta^2(1-\nu)\frac{\partial^2 V}{\partial Y^2}+(1-2\nu)\frac{\partial^2 V}{\partial Z^2}+\alpha\beta\frac{\partial^2 W}{\partial Y\,\partial Z}$$
$$=2(1+\nu)(2\nu-1)\frac{\rho\omega^2}{E}V \tag{13b}$$

$$\gamma\frac{\partial^2 U}{\partial X\,\partial Z}+\gamma\frac{\partial^2 V}{\partial Y\,\partial Z}+\gamma^2(1-2\nu)\frac{\partial^2 W}{\partial X^2}+\beta^2(1-2\nu)\frac{\partial^2 W}{\partial Y^2}+2(1-\nu)\frac{\partial^2 W}{\partial Z^2}$$
$$=2(1+\nu)(2\nu-1)\frac{\rho\omega^2}{E}W. \tag{13c}$$

Using similar procedures, the stress–displacement equations [equations (8)] can be normalized into the following:

$$\sigma_X=\gamma(1-\nu)\frac{\partial U}{\partial X}+\gamma\nu\frac{\partial V}{\partial Y}+\nu\frac{\partial W}{\partial Z} \tag{14}$$

$$\sigma_Y=\gamma\nu\frac{\partial U}{\partial X}+\gamma(1-\nu)\frac{\partial V}{\partial Y}+\nu\frac{\partial W}{\partial Z} \tag{15}$$

$$\sigma_Z=\gamma\nu\frac{\partial U}{\partial X}+\gamma\nu\frac{\partial V}{\partial Y}+(1-\nu)\frac{\partial W}{\partial Z} \tag{16}$$

$$\alpha^2\tau_{XY}=\alpha^2\frac{\partial U}{\partial Y}+\frac{\partial V}{\partial X} \tag{17}$$

$$\gamma\tau_{XZ}=\gamma\frac{\partial W}{\partial X}+\frac{\partial U}{\partial Z} \tag{18}$$

$$\beta\tau_{YZ}=\frac{\partial V}{\partial Z}+\alpha\beta\frac{\partial W}{\partial Y}. \tag{19}$$

According to the differential quadrature method, the normalized governing equations [equations (13)] can be discretized into the following forms:

$$2\gamma^2(1-\nu)\sum_{l=1}^{N_X}A_{il}^{(2)}U_{ljk}+\beta^2(1-2\nu)\sum_{m=1}^{N_Y}B_{jm}^{(2)}U_{imk}+(1-2\nu)\sum_{n=1}^{N_Z}C_{kn}^{(2)}U_{ijn}$$
$$+\gamma^2\sum_{l=1}^{N_X}A_{il}^{(1)}\sum_{m=1}^{N_Y}B_{jm}^{(1)}V_{lmk}+\gamma\sum_{l=1}^{N_X}A_{il}^{(1)}\sum_{n=1}^{N_Z}C_{kn}^{(1)}W_{ljn}$$
$$=2c^2(1+\nu)(2\nu-1)\frac{\rho\omega^2}{E}U_{ijk} \tag{20a}$$

$$\beta^2 \sum_{l=1}^{N_X} A_{il}^{(1)} \sum_{m=1}^{N_Y} B_{jm}^{(1)} U_{lmk} + \gamma^2(1-2\nu) \sum_{l=1}^{N_X} A_{il}^{(2)} V_{ljk} + 2\beta^2(1-\nu) \sum_{m=1}^{N_Y} B_{jm}^{(2)} V_{imk}$$

$$+(1-2\nu) \sum_{n=1}^{N_Z} C_{kn}^{(2)} V_{ijn} + \alpha\beta \sum_{m=1}^{N_Y} B_{jm}^{(1)} \sum_{n=1}^{N_Z} C_{kn}^{(1)} W_{imn})$$

$$= 2(1+\nu)(2\nu-1) \frac{\rho\omega^2}{E} V_{ijk} \tag{20b}$$

$$\gamma \sum_{l=1}^{N_X} A_{il}^{(1)} \sum_{n=1}^{N_Z} C_{kn}^{(1)} U_{ljn} + \gamma \sum_{m=1}^{N_Y} B_{jm}^{(1)} \sum_{n=1}^{N_Z} C_{kn}^{(1)} V_{imn} + \gamma^2(1-2\nu) \sum_{l=1}^{N_X} A_{il}^{(2)} W_{ljk}$$

$$+\beta^2(1-2\nu) \sum_{m=1}^{N_Y} B_{jm}^{(2)} W_{imk} + 2(1-\nu) \sum_{n=1}^{N_Z} C_{kn}^{(2)} W_{ijn}$$

$$= 2(1+\nu)(2\nu-1) \frac{\rho\omega^2}{E} W_{ijk} \tag{20c}$$

$$\sigma_X = \gamma(1-\nu) \sum_{l=1}^{N_X} A_{il}^{(1)} U_{ljk} + \gamma\nu \sum_{m=1}^{N_Y} B_{jm}^{(1)} V_{imk} + \nu \sum_{n=1}^{N_Z} C_{kn}^{(1)} W_{ijn} \tag{21}$$

$$\sigma_Y = \gamma\nu \sum_{l=1}^{N_X} A_{il}^{(1)} U_{ljk} + \gamma(1-\nu) \sum_{m=1}^{N_Y} B_{jm}^{(1)} V_{imk} + \nu \sum_{n=1}^{N_Z} C_{kn}^{(1)} W_{ijn} \tag{22}$$

$$\sigma_Z = \gamma\nu \sum_{l=1}^{N_X} A_{il}^{(1)} U_{ljk} + \gamma\nu \sum_{m=1}^{N_Y} B_{jm}^{(1)} V_{imk} + (1-\nu) \sum_{n=1}^{N_Z} C_{kn}^{(1)} W_{ijn} \tag{23}$$

$$\alpha^2 \tau_{XY} = \alpha^2 \sum_{m=1}^{N_Y} B_{jm}^{(1)} U_{imk} + \sum_{l=1}^{N_X} A_{il}^{(1)} V_{ljk} \tag{24}$$

$$\gamma \tau_{XZ} = \gamma \sum_{l=1}^{N_X} A_{il}^{(1)} W_{ljk} + \sum_{n=1}^{N_Z} C_{kn}^{(1)} U_{ijn} \tag{25}$$

$$\beta \tau_{YZ} = \sum_{n=1}^{N_Z} C_{kn}^{(1)} V_{ijn} + \alpha\beta \sum_{m=1}^{N_Y} B_{jm}^{(1)} W_{imk}. \tag{26}$$

4.3. NORMALIZATION AND DISCRETIZATION OF THE BOUNDARY CONDITIONS

By substituting the non-dimensional parameters, [equations (12)] into the boundary conditions [equations (9)–(11)] will give their normalized form. Below are the examples of the normalized form of the edge boundary conditions at $X =$ constant and boundary conditions for the top and bottom surfaces of the plate.

Normalized clamped boundary condition (C):

$$U = 0; \qquad V = 0; \qquad W = 0. \tag{27}$$

Simply supported boundary condition (S):

$$\gamma(1-\nu)\frac{\partial U}{\partial X} + \gamma\nu\frac{\partial V}{\partial Y} + \nu\frac{\partial W}{\partial Z} = 0; \qquad V = 0; \qquad W = 0. \tag{28a–c}$$

Free surface boundary conditions:

$$\gamma\nu\frac{\partial U}{\partial X} + \gamma\nu\frac{\partial V}{\partial Y} + (1-\nu)\frac{\partial W}{\partial Z} = 0 \tag{29a}$$

$$\gamma\frac{\partial W}{\partial X} + \frac{\partial U}{\partial Z} = 0 \tag{29b}$$

$$\frac{\partial V}{\partial Z} + \alpha\beta\frac{\partial W}{\partial Y} = 0. \tag{29c}$$

According to the differential quadrature procedure, the above equations [equations (27)–(29)] can be discretized into the following:

Discretized clamped boundary condition (C):

$$U_{ijk} = 0; \qquad V_{ijk} = 0; \qquad W_{ijk} = 0. \tag{30}$$

Simply supported boundary condition (S):

$$\gamma(1-\nu)\sum_{l=1}^{N_X} A_{il}^{(1)} U_{ljk} + \gamma\nu\sum_{m=1}^{N_Y} B_{jm}^{(1)} V_{imk} + \nu\sum_{n=1}^{N_Z} C_{kn}^{(1)} W_{ijn} = 0; \tag{31a}$$

$$V_{ijk} = 0; \qquad W_{ijk} = 0. \tag{31b–c}$$

Free surface boundary condition:

$$\gamma\nu\sum_{l=1}^{N_X} A_{il}^{(1)} U_{ljk} + \gamma\nu\sum_{m=1}^{N_Y} B_{jm}^{(1)} V_{imk} + (1-\nu)\sum_{n=1}^{N_Z} C_{kn}^{(1)} W_{ijn} = 0; \tag{32a}$$

$$\gamma\sum_{l=1}^{N_X} A_{il}^{(1)} W_{ljk} + \sum_{n=1}^{N_Z} C_{kn}^{(1)} U_{ijn} = 0; \tag{32b}$$

$$\sum_{n=1}^{N_Z} C_{kn}^{(1)} V_{ijn} + \alpha\beta\sum_{m=1}^{N_Y} B_{jm}^{(1)} W_{imk} = 0. \tag{32c}$$

4.4. SOLUTION PROCEDURE

From the above procedures, one can derive the general form of eigenvalue equation as follows:

$$\mathbf{DU} = \lambda \mathbf{EU} \tag{33}$$

in which

$$\mathbf{U} = \begin{bmatrix} U_{ijk} \\ V_{ijk} \\ W_{ijk} \end{bmatrix} \tag{34}$$

where **D** and **E** are matrices derived from the governing equations [equations (13)]; **U** is the displacement matrix.

In the above eigenvalue equation, λ is the non-dimensional frequency parameter used in this paper. It is defined as $\lambda = (\omega b^2/\pi^2)\sqrt{\rho h/D}$ where D is the flexural rigidity of the plate.

The determinant of the matrix to be solved for a solution domain with grid size of $N_x \times N_y \times N_z$ is $(3 \times N_x \times N_y \times N_z)$. This is because for every point in the solution domain, there are three conditions that need to be satisfied, be it the three governing equations or the three equations describing the particular boundary condition under consideration.

In forming the system of equations, the points on the six faces of the plate are described by the boundary conditions whereas the points inside the plate are described by the governing equations. If $N_x = N_y = N_z = N$, the solution domain of $N \times N \times N$ points has $(4N^2 - 6N + 4)$ points being described by the boundary conditions. In another words, there are $(N-2)^3$ points in the solutions domain that are described by the three governing equations.

5. RESULTS AND DISCUSSION

In this discussion, symbols are used for plates subject to different boundary condition. For example, a plate with all edges simply supported is denoted by SSSS while all edges clamped is denoted by CCCC. A SCSC plate is a plate with the edges $X = 0$ and 1 simply supported and edges $Y = 0$ and 1 clamped.

When the solution domain is discretized, one needs to determine the mesh patterns to be used. The two commonly used mesh patterns are the uniform mesh pattern and the cosine mesh pattern. The uniform mesh pattern divides the solution domain into points equidistant to one another. The cosine mesh pattern, however, divides the solution domain into points following a cosine function. Below is the formula showing the division of the axes into cosine mesh pattern:

$$\Theta(i) = 0{\cdot}5\left(1 - \frac{\cos{(i-1)} \times \pi}{N-1}\right) \tag{35}$$

where $\Theta(i)$ can be the $x(i)$, $y(i)$ or $z(i)$ co-ordinate of the ith points considered.

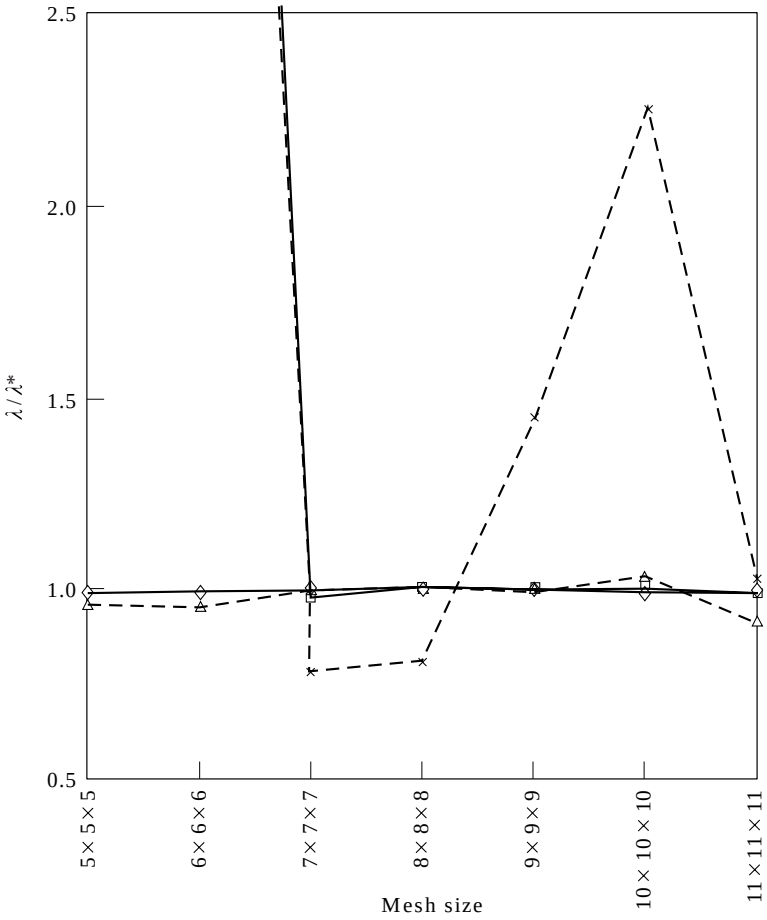

Figure 2. Convergence study of the frequency parameter, $\lambda = (\omega b^2/\pi^2)\sqrt{\rho h/D}$, of a square SSSS plate under different mesh pattern. $a/b = 1$, $c/b = 0{\cdot}01$, $v = 0{\cdot}3$, λ^* ——, Exact Classical Plate theory solution, reference [40]. ◇, Mode 1, cosine mesh; △, Mode 1, uniform mesh; □, Mode 6, cosine mesh; ×, Mode 6, uniform mesh.

A very important condition to be met before determining the mesh pattern to be used is the convergence of the solution. This should take precedence in the study of numerical methods. Figures 2 to 5 are employed to study the mesh pattern together with the convergence characteristics. The first and the sixth modes are chosen in this study as they are representative of the lower and the higher modes. In these figures, the DQ solution using both the uniform mesh and the cosine mesh is presented. The frequency parameter, $\lambda = (\omega b^2/\pi^2)\sqrt{\rho h/D}$, in these figures is normalized using available results. As in Figure 2, the DQ solution is normalized using exact solutions from the classical plate theory [40]. Due to the two theories being different, one cannot conduct an accuracy study; only the convergence study is done. The frequency parameter in Figures 3 and 4 are normalized using an exact three-dimensional solution [30]. In this aspect, a convergence study as well as preliminary accuracy study is shown. The frequency parameter in Figure 5 is normalized using the three-dimensional solution derived from the *p*-Ritz method

[41]. Though it is also a numerical solution, it is considered to be an accurate solution.

In Figure 2, one can deduce that regardless of the mesh pattern, the first mode begins to converge starting from the mesh size of $5 \times 5 \times 5$. The solution from the cosine mesh proves faster convergence after increasing the mesh size beyond $9 \times 9 \times 9$. For the higher mode solution using the cosine mesh, acceptable convergence only starts at mesh size $7 \times 7 \times 7$. As for the results from the uniform mesh, one can only conclude that even at a mesh size of $11 \times 11 \times 11$, the results are still not convergent. It is predicted that further refinement of the mesh may yield convergent results.

Figure 3 shows the convergence and accuracy study of the first and the sixth modes of a fully simply supported square plate with a thickness to width ratio of $c/b = 0{\cdot}1$. In the figure, the convergence of the first mode, regardless of mesh pattern, begins from the mesh size of $5 \times 5 \times 5$. Accurate results are obtained from mesh size $8 \times 8 \times 8$ onwards. It is shown that the convergent results of the first mode solution using the cosine mesh pattern yield more accurate results than

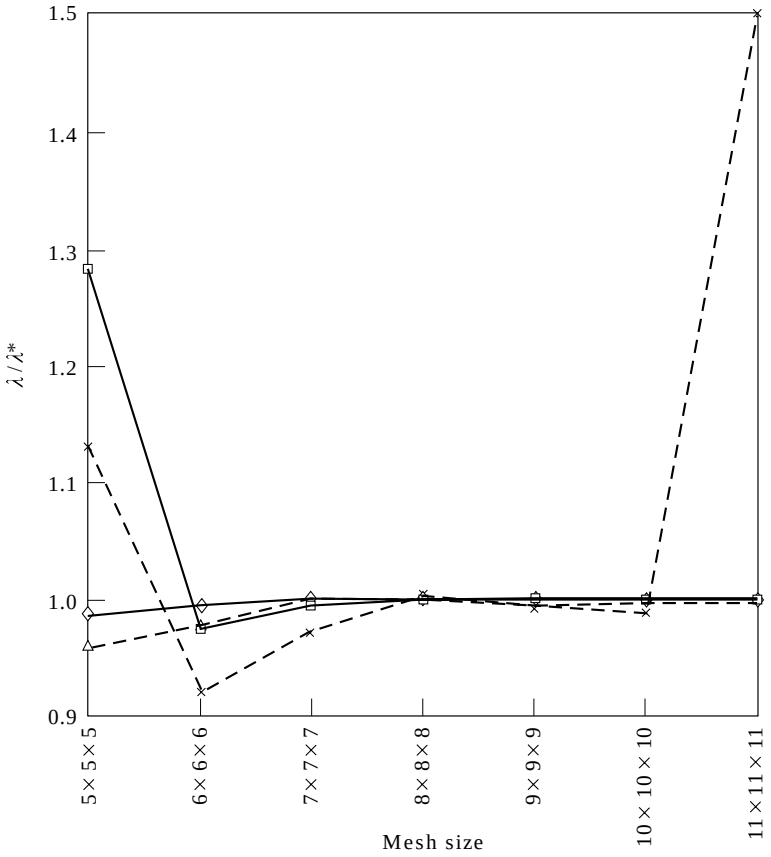

Figure 3. Convergence and accuracy study of the frequency parameter, $\lambda = (\omega b^2/\pi^2)\sqrt{\rho h/D}$, of a square SSSS plate under different mesh pattern. $a/b = 1$, $c/b = 0{\cdot}1$, $\nu = 0{\cdot}3$, λ^* ——, Exact three-dimensional solution, reference [30]. ◇, Mode 1, cosine mesh; △, Mode 1, uniform mesh; □, Mode 6, cosine mesh; ×, Mode 6, uniform mesh.

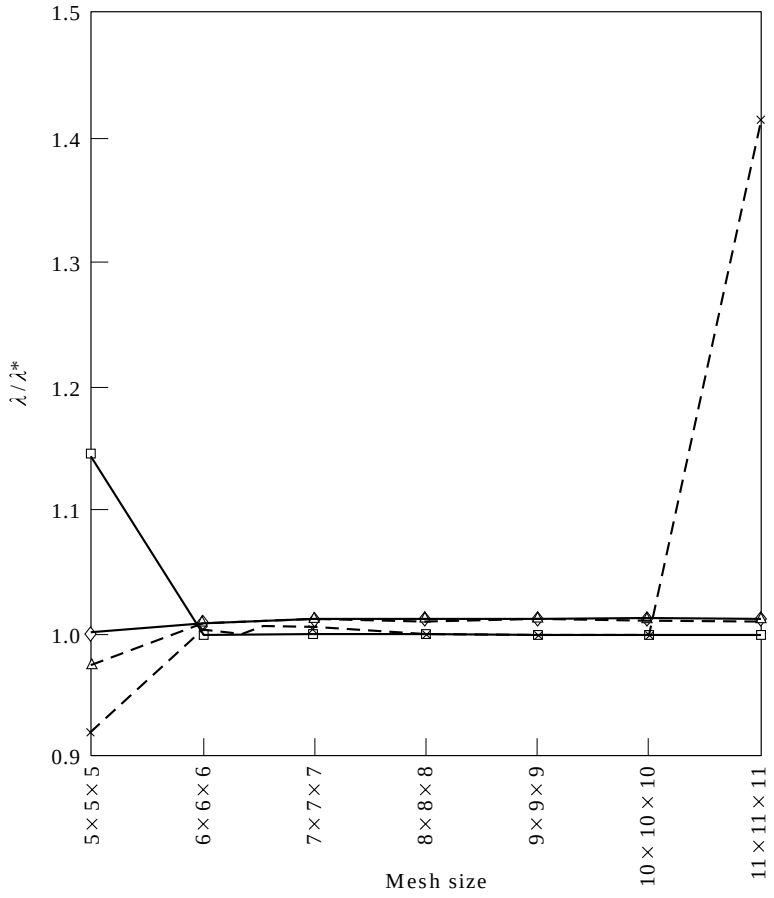

Figure 4. Convergence and accuracy study of the frequency parameter, $\lambda = (\omega b^2/\pi^2)\sqrt{\rho h/D}$, of a square SSSS plate under different mesh pattern. $a/b = 1$, $c/b = 0{\cdot}2$, $\nu = 0{\cdot}3$, λ^* ——, Exact three-dimensional solution, reference [30]. ◇, Mode 1, cosine mesh; △, Mode 1, uniform mesh; □, Mode 6, cosine mesh; ×, Mode 6, uniform mesh.

those generated from the uniform mesh pattern. As for the case of the sixth mode, the results of cosine mesh converge to the accurate solution at mesh size $8 \times 8 \times 8$ since the normalized result is unity; the results generated using a uniform mesh pattern converges to the accurate result at mesh size $8 \times 8 \times 8$ but diverges at a mesh size of $10 \times 10 \times 10$.

Similar to Figure 3, Figure 4 shows the convergence and accuracy study of the frequency parameters of a fully simply supported square plate, this time with $c/b = 0{\cdot}2$. It is seen that the first mode converges to the similar value at mesh size $5 \times 5 \times 5$. It is also noted that both the cosine and the uniform mesh patterns yield a result which is slightly higher than the exact solution as the curve is higher than unity. For the sixth mode, convergence also starts at mesh size $5 \times 5 \times 5$. When the result is generated from the cosine mesh, the convergence is stable and accurate even up to mesh size $11 \times 11 \times 11$. This is not so for the uniform mesh. Though its results converge in similar fashion as the cosine mesh pattern, they diverge at

mesh size $11 \times 11 \times 11$. It should be added that such divergence is about 41%, hence rendering the results inaccurate.

The convergence study of DQ results using cosine mesh and uniform mesh for a thick SSSS square plate, $c/b = 0{\cdot}5$, is shown in Figure 5. It is observed that at mesh size $7 \times 7 \times 7$, the lower and higher modes of the cosine mesh results converge to the correct result. Mode 1 of the DQ results using the uniform mesh also have the same convergence pattern. This is not so for the higher mode. One can observe that DQ results using the uniform mesh give rather unstable results until mesh size $10 \times 10 \times 10$ is reached.

At this point of the study one can conclude that the uniform mesh pattern is able to give rather reliable results for the lower mode of vibration if the plate is moderately thick; its results are unstable for the case of the thin plate. For the case of the moderately thick plate, its solution is reliable only at mesh sizes ranging from $8 \times 8 \times 8$ to $10 \times 10 \times 10$. On the contrary, the cosine mesh pattern yields stable and accurate results for plates of different thickness to width ratios. Its

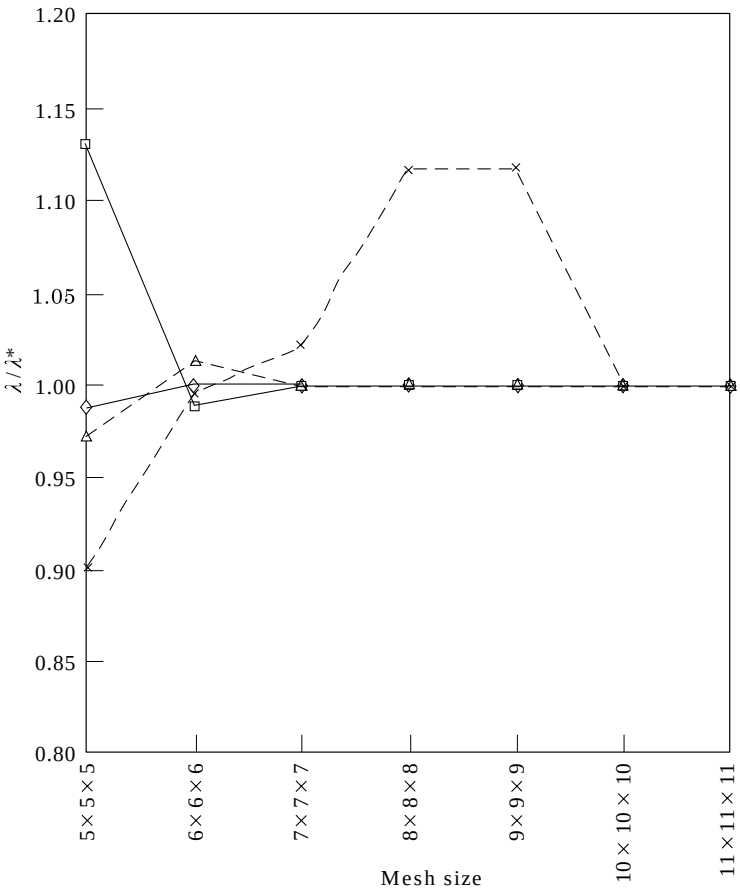

Figure 5. Convergence study of the frequency parameter, $\lambda = (\omega b^2/\pi^2)\sqrt{\rho h/D}$, of a square SSSS plate under different mesh pattern. $a/b = 1$, $c/b = 0{\cdot}01$, $v = 0{\cdot}3$, λ^* ——, three-dimensional p-Ritz solution, reference [41]. ◇, Mode 1, cosine mesh; △, Mode 1, uniform mesh; □, Mode 6, cosine mesh; ×, Mode 6, uniform mesh.

results are also stable. Due to the above conclusion, the cosine mesh pattern shall be used for the remaining part of the study.

To conduct a convergence study in detail, sample results are chosen and are presented in Tables 1–3. In these tables, the first eight modal solutions of the SSSS, CCCC and SCSC plates are shown.

As with many other numerical methods, the solution for plates with the lowest thickness to width ratio has the most difficulty in converging. Due to this inherent difficulty, the convergence of the frequency parameter of thin square plates with $c/b = 0{\cdot}01$ shall be studied first. This is shown in Table 1. It can be noted that the correct order of magnitude for the higher modal solution (starting from mode 5) is reached only beyond mesh size $7 \times 7 \times 7$. This is true for all the combinations of boundary conditions considered. For the case of the SSSS plate, the 3rd significant figure convergent solution is reached at mesh size $9 \times 9 \times 9$; for CCCC and SCSC plates, the 3rd significant figure convergent solution is reached at mesh size $10 \times 10 \times 10$.

Table 2 shows the convergence of the frequency parameters of moderately thick square plates subject to the same set of boundary conditions considered above. For a SSSS square plate, the 3rd significant figure convergent solution is reached at mesh size $8 \times 8 \times 8$; for a CCCC square plate, the 3rd significant figure convergent solution is reached at mesh size $10 \times 10 \times 10$; for a SCSC square plate, the 3rd significant figure convergent solution is reached at mesh size $9 \times 9 \times 9$. One can also see that the convergence of the lower modes is better than the higher modes.

Table 3 shows the convergence study of a moderately thick rectangular plate ($c/b = 0{\cdot}25$) with an aspect ratio of $a/b = 2{\cdot}0$. Similar to the above, the first eight modal solutions shall be analyzed. It is observed that the SSSS plate has a convergent result at mesh size $9 \times 9 \times 9$; for the case of a CCCC and SCSC plate, the convergent result is at mesh size $10 \times 10 \times 10$.

Hence, the deduction drawn from the above convergence study is under similar a/b or c/b; the SSSS plate converges the earliest whereas the CCCC plate converges the slowest.

In order to verify the accuracy of the DQ method in solving the three-dimensional elastic plate problem, an accuracy study is conducted. Such a study compares the current DQ solution with published results. As far as possible, the authors try to compare the current results with the exact solution, preferably from a three-dimensional theory. In this study, the percentage deviation of the DQ results from the published solution is determined based on the following expressions:

$$\% \text{ Deviation} = \left| \left(\frac{\text{Present solution} - \text{Published solution}}{\text{Published solution}} \right) \right| \times 100\%. \quad (36)$$

Table 4 shows the comparison study of the frequency parameter of thin and thick square plates subject to SSSS boundary condition. In this study, the thin plate, $c/b = 0{\cdot}01$, is compared with the exact classical plate solution [40] and the three-dimensional p-Ritz solution [41]. Solutions from other plate theories are also

TABLE 1

Convergence of frequency parameters, $\lambda = (\omega b^2/\pi^2)\sqrt{\rho h/D}$ of thin square plates, $(a/b = 1{\cdot}0, c/b = 0{\cdot}01)$, under different boundary conditions

Grid points $X \times Y \times Z$	Mode sequence number							
	1	2	3	4	5	6	7	8
				SSSS				
$5 \times 5 \times 5$	1·9757	65·083	65·083	83·155	83·155	90·626	117·63	143·86
$6 \times 6 \times 6$	1·9832	4·8814	4·8824	7·7702	65·226	65·226	92·288	128·67
$7 \times 7 \times 7$	2·0019	4·9443	4·9475	7·9148	9·7636	9·7642	12·682	12·683
$8 \times 8 \times 8$	2·0084	5·0031	5·0061	7·9989	10·018	10·018	13·017	13·018
$9 \times 9 \times 9$	1·9952	4·9977	5·0081	7·9957	10·024	10·029	13·011	13·012
$10 \times 10 \times 10$	1·9838	4·9818	5·0099	7·9914	10·027	10·028	13·000	13·006
$11 \times 11 \times 11$	2·0028	4·9878	5·0065	7·9873	9·9745	9·9807	12·966	12·971
				CCCC				
$5 \times 5 \times 5$	3·7933	117·53	117·53	125·65	125·65	158·73	166·17	176·22
$6 \times 6 \times 6$	3·8135	7·9068	7·9083	11·215	125·51	125·51	148·18	182·72
$7 \times 7 \times 7$	3·6949	8·0937	8·0955	11·607	14·954	15·072	17·812	17·812
$8 \times 8 \times 8$	3·6896	7·4811	7·4840	11·022	15·637	15·752	18·462	18·463
$9 \times 9 \times 9$	3·6648	7·4730	7·4758	11·021	13·332	13·384	16·716	16·717
$10 \times 10 \times 10$	3·6671	7·4599	7·4705	10·995	13·367	13·430	16·748	16·748
$11 \times 11 \times 11$	3·6516	7·4505	7·4664	10·975	13·356	13·419	16·738	16·742
				SCSC				
$5 \times 5 \times 5$	3·0228	65·083	83·189	115·82	117·50	122·74	143·86	143·95
$6 \times 6 \times 6$	3·0374	5·4561	7·5219	9·6475	65·226	115·16	122·88	128·67
$7 \times 7 \times 7$	2·9590	5·5197	7·7106	9·9331	10·140	14·087	14·769	16·730
$8 \times 8 \times 8$	2·9633	5·5720	7·0537	9·6150	10·387	14·255	15·455	17·146
$9 \times 9 \times 9$	2·9335	5·5559	7·0531	9·6168	10·395	13·065	14·243	15·655
$10 \times 10 \times 10$	2·9485	5·5533	7·0439	9·5918	10·386	13·114	14·234	15·693
$11 \times 11 \times 11$	2·9518	5·5439	7·0460	9·5914	10·336	13·114	14·190	15·689

presented for comparison and verification purposes. When the present solution is compared with the classical theory, the percentage deviation is less than one percent for all of the first eight modes. The highest deviation is for mode 6 which amounts to 0·29% whereas the lowest deviation comes from mode 2 which amounts to 0·046%. When the present solution is compared with the three-dimensional p-Ritz solution [41], the largest deviation also comes from mode 6 with a value of 0·46%; the least deviation comes from mode 7 with a value of 0·31%. It should be commented that the fundamental mode has lower percentage deviation when compared with the Ritz solution.

For a square SSSS plate with $c/b = 0{\cdot}1$, one can observe that the p-Ritz method has the same value as the exact three-dimensional solution [30]. This is true for the first eight modes in study except for modes 4 and 5 where the exact solution is not available. In this case, the accuracy study shall be done by comparing the DQ solution with the exact solution for mode 1 to 8 except mode 4 and 5 in which the comparison shall be made with the solution form the p-Ritz method [41]. In the comparison analysis, the DQ solution for mode 1 has the same value as the exact solution; modes 4 and 5 yields zero percent deviation when compared with the p-Ritz method [41]. Both mode 7 and mode 8 have the highest deviation of 0·36% when compared with the exact solution [30].

TABLE 2

Convergence of frequency parameters, $\lambda = (\omega b^2/\pi^2)\sqrt{\rho h/D}$, *of thick rectangular plates,* $(a/b = 1{\cdot}0, c/b = 0{\cdot}25)$ *under different boundary conditions*

Grid points $X \times Y \times Z$	Mode sequence number							
	1	2	3	4	5	6	7	8
				SSSS				
$5 \times 5 \times 5$	1·6636	2·6033	2·6033	3·6242	4·4805	4·4805	5·7545	5·7545
$6 \times 6 \times 6$	1·6807	2·6091	2·6091	3·4963	3·4963	3·6915	4·9446	5·1470
$7 \times 7 \times 7$	1·6832	2·6094	2·6094	3·5490	3·5490	3·6922	5·0333	5·2210
$8 \times 8 \times 8$	1·6830	2·6094	2·6094	3·5556	3·5556	3·6902	5·0389	5·2187
$9 \times 9 \times 9$	1·6830	2·6094	2·6094	3·5529	3·5529	3·6902	5·0365	5·2188
$10 \times 10 \times 10$	1·6830	2·6094	2·6094	3·5523	3·5523	3·6902	5·0358	5·2187
				CCCC				
$5 \times 5 \times 5$	2·4859	5·0269	5·0269	5·2934	5·2934	6·3493	7·1186	7·3244
$6 \times 6 \times 6$	2·4777	4·2063	4·2063	5·0278	5·0278	5·5482	5·9314	7·2856
$7 \times 7 \times 7$	2·4607	4·1826	4·1826	5·0260	5·0260	5·5565	5·9509	6·2216
$8 \times 8 \times 8$	2·4578	4·1687	4·1687	5·0251	5·0251	5·5449	5·9506	6·3315
$9 \times 9 \times 9$	2·4563	4·1666	4·1666	5·0242	5·0242	5·5421	5·9505	6·2692
$10 \times 10 \times 10$	2·4552	4·1656	4·1656	5·0233	5·0233	4·5412	5·9504	6·2714
				SCSC				
$5 \times 5 \times 5$	2·0938	2·6033	4·5908	4·6336	4·8929	5·1581	5·7545	6·5752
$6 \times 6 \times 6$	2·0996	2·6091	3·6323	4·0548	4·6135	4·9049	5·1470	5·2246
$7 \times 7 \times 7$	2·0919	2·6094	3·6769	4·0415	4·6156	4·9035	5·2210	5·2787
$8 \times 8 \times 8$	2·0902	2·6094	3·6831	4·0293	4·6152	4·9019	5·2187	5·2777
$9 \times 9 \times 9$	2·0892	2·6094	3·6798	4·0276	4·6148	4·9017	5·2188	5·2748
$10 \times 10 \times 10$	2·0886	2·6094	3·6790	4·0269	4·6144	4·9014	5·2187	5·2741

TABLE 3

Convergence of frequency parameters, $\lambda = (\omega b^2/\pi^2)\sqrt{\rho h/D}$, of thick rectangular plates, $(a/b = 2{\cdot}0, c/b = 0{\cdot}25)$ under different boundary conditions

Grid points $X \times Y \times Z$	Mode sequence number 1	2	3	4	5	6	7	8
				SSSS				
$5 \times 5 \times 5$	1·0976	1·3017	2·2456	2·6033	2·8772	2·8833	3·6444	3·6719
$6 \times 6 \times 6$	1·1097	1·3045	1·6626	2·5735	2·6091	2·9179	3·0712	3·4819
$7 \times 7 \times 7$	1·1128	1·3047	1·6806	2·4757	2·6094	2·6105	2·9183	3·1268
$8 \times 8 \times 8$	1·1126	1·3047	1·6838	2·5372	2·6093	2·6094	2·9174	3·1354
$9 \times 9 \times 9$	1·1125	1·3047	1·6833	2·5316	2·6094	2·6094	2·9173	3·1319
$10 \times 10 \times 10$	1·1125	1·3047	1·6829	2·5289	2·6094	2·6094	2·9174	3·1312
				CCCC				
$5 \times 5 \times 5$	1·8329	2·9940	3·3715	3·9371	4·5271	4·9806	4·9849	5·5352
$6 \times 6 \times 6$	1·8209	2·2856	3·3741	3·7914	4·1181	4·4055	4·5181	4·7395
$7 \times 7 \times 7$	1·8064	2·2755	3·0388	3·3713	3·7605	4·1111	4·5127	4·6515
$8 \times 8 \times 8$	1·8036	2·2572	3·0576	3·3711	3·7436	4·0057	4·0951	4·5119
$9 \times 9 \times 9$	1·8024	2·2558	2·9939	3·3703	3·7417	4·0781	4·0926	4·5110
$10 \times 10 \times 10$	1·8013	2·2549	2·9967	3·3702	3·7407	3·9289	4·0917	4·5101
				SCSC				
$5 \times 5 \times 5$	1·1809	1·3017	2·6622	2·8772	3·0827	3·6719	3·6729	4·1883
$6 \times 6 \times 6$	1·1935	1·3045	1·8839	2·5735	3·0921	3·0981	3·5460	3·9673
$7 \times 7 \times 7$	1·1950	1·3047	1·8907	2·6105	2·7949	3·0989	3·1465	3·6130
$8 \times 8 \times 8$	1·1933	1·3047	1·8744	2·6093	2·8307	3·0984	3·1546	3·6173
$9 \times 9 \times 9$	1·1930	1·3047	1·8734	2·6094	2·7680	3·0983	3·1510	3·6136
$10 \times 10 \times 10$	1·1925	1·3047	1·8731	2·6094	2·7715	3·0983	3·1501	3·6128

The final comparison study for the SSSS square plate is done for a plate with $c/b = 0{\cdot}2$. In this case, modes 1, 4, 5, 6 and 7 of the DQ solution shall be used to compare with the exact solution [30]. This is because the exact solution for modes 2, 3, and 8 is unavailable. The percentage deviations of modes 1, 4, 5, 6 and 7 when compared with the exact solution are 1·145%, 0·205%, 0·205%, 0·002% and 0·011% respectively. The DQ solution for modes 2, 3 and 8 shall be compared with the p-Ritz method [41]. It is discovered that modes 2 and 3 have zero deviation whereas modes 5 and 8 have 0·205% and 0·003% deviations respectively.

From the above analysis of Table 4, one can conclude that the DQ solution is accurate in solving the SSSS plate problem. Generally, the accuracy for the cases studied can be limited to $<1{\cdot}5\%$ deviation from the exact solution [30]. It is also noticed that the solution of the first order plate theory [42] has the most deviation from the exact three-dimensional solution [30]. This is followed by the higher order theory [43]. It is also noticed that the numerical three-dimensional results considered deviate less when compared with the exact three-dimensional solution. Hence, it can be generally regarded that the numerical three-dimensional results are still more accurate than the results generated by other plate theories. Its uniqueness proves the need for three-dimensional numerical solution.

TABLE 4

Comparison of frequency parameters, $\lambda = (\omega b^2/\pi^2)\sqrt{\rho h/D}$, for thin and thick square plates with SSSS boundary condition

Thickness ratio, c/b	Solution method	Mode sequence number							
		1	2	3	4	5	6	7	8
0·01	Classical theory[a]	2·0	5·0	5·0	8·0	10·0	10·0	13·0	13·0
	Midlin theory[b]	1·9992	4·9954	4·9954	7·9882	9·9816	9·9816	—	—
	3-D Ritz solutions[c]	1·9993	4·9956	4·9956	7·9888	9·9826	9·9826	12·9710	12·9710
	Present 3-D solutions	1·9952	4·9977	5·0081	7·9957	10·0240	10·0290	13·0110	13·0120
0·1	Midlin theory[b]	1·9311	4·6048	4·6048	—	—	7·0637	8·6049	8·6049
	Midlin theory[d]	1·931	4·605	4·605	—	—	7·064	8·605	8·605
	Higher order theory[e]	1·9353	4·6222	4·6222	—	—	7·1036	8·6609	8·6609
	3-D exact solutions[f]	1·9342	4·6222	4·6222	—	—	7·1030	8·6617	8·6617
	3-D Ritz solutions[c]	1·9342	4·6222	4·6222	6·5234	6·5234	7·1030	8·6617	8·6617
	Present 3-D solutions	1·9342	4·6250	4·6250	6·5234	6·5234	7·1064	8·6932	8·6932
0·2	Midlin theory[d]	1·7659	—	—	3·8576	3·8576	—	5·5729	6·5809
	Higher order theory[e]	1·7558	—	—	3·8991	3·8991	—	5·6526	6·6867
	3-D exact solutions[f]	1·7557	—	—	3·8991	3·8991	4·6128	5·6527	—
	3-D Ritz solutions[c]	1·7558	3·2617	3·2617	3·8991	3·8991	4·6128	5·6524	6·5234
	Present 3-D solutions	1·7758	3·2617	3·2617	3·8999	3·8999	4·6127	5·6533	6·5236

[a] Reference [40]; [b] reference [42]; [c] reference [41]; [d] reference [47]; [e] reference [43]; [f] reference [30].

TABLE 5

Comparison of frequency parameters, $\lambda = (\omega b^2/\pi^2)\sqrt{\rho h/D}$, for thin and thick square plates with CCCC boundary condition

Thickness ratio, c/b	Solution method	Mode sequence number							
		1	2	3	4	5	6	7	8
0·01	Classical theory[a]	3·6459	7·4370	7·4370	10·963	13·366	13·366	16·718	16·718
	Midlin theory[b]	3·6421	7·4254	7·4254	10·951	13·294	13·356	—	—
	3-D Ritz solutions[c]	3·6492	7·4352	7·4352	10·953	13·315	13·379	16·682	16·682
	Present 3-D solutions	3·6671	7·4599	7·4705	10·995	13·367	13·430	16·748	16·748
0·1	Midlin theory[b]	3·3099	6·3249	6·3249	8·8977	10·455	10·544	—	—
	Midlin theory[d]	3·2954	6·2858	6·2858	8·8098	10·379	10·478	12·553	12·553
	3-D Ritz solutions[c]	3·3184	6·3402	6·3402	8·8961	10·490	10·590	12·519	12·519
	Present 3-D solutions	3·3282	6·3547	6·3547	8·9135	10·493	10·592	12·524	12·524
0·2	3-D Ritz solutions[c]	2·7247	4·7706	4·7706	6·2727	6·2727	6·4163	7·3219	7·4225
	Present 3-D solutions	2·7288	4·7762	4·7762	6·2754	6·2754	6·4224	7·3254	7·4258

[a] reference [44]; [b] reference [45]; [c] reference [41]; [d] reference [46].

The comparison study is done for a CCCC square plate as shown in Table 5. For the case of thin plate, $c/b = 0{\cdot}01$, one can deduce that the deviation of the DQ results from that of the classical theory [44] is $<0{\cdot}6\%$. When the DQ solution is compared with that of the three-dimensional p-Ritz method [41], the deviation is $0{\cdot}5\%$. For the case of plates with $c/b = 0{\cdot}1$, the deviation of the DQ solution from that of the p-Ritz method [41] is $<0{\cdot}3\%$. When the plate's $c/b = 0{\cdot}2$, the deviation with Ritz method is $<0{\cdot}2\%$. Hence, one can safely say the DQ solution yields accurate results.

6. CONCLUSIONS

This paper verifies that the DQ method is able to solve problems related to three-dimensional vibration of plates with a high degree of accuracy. The discussions in the previous section also allows the following conclusions to be drawn. Firstly, the cosine mesh pattern is a more desirable mesh for solving three-dimensional plate vibration problems. It is also concluded that three-dimensional numerical solutions for plate problems yield highly accurate solutions thus complementing solutions derived from other plate theories like the first order plate theory and the higher order plate theories. This gives rise to a need for further studies into this field of research.

REFERENCES

1. R. E. Bellman and J. Casti 1971 *Journal of Mathematical Analysis and Applications* **34**, 235–238. Differential quadrature and long-term integration.
2. R. E. Bellman, B. G. Kashef and J. Casti 1972 *Journal of Computational Physics* **10**, 40–52. Differential quadrature: a technique for the rapid solution of nonlinear partial differential equations.
3. R. E. Bellman 1973 *Methods of Nonlinear Analysis*. New York: Academic Press.
4. C. W. Bert, S. K. Jang and A. G. Striz 1988 *American Institute of Aeronautics and Astronautics Journal* **26**, 612–618. Two new approximate methods for analyzing free vibration of structural components.
5. F. Civan and C. M. Sliepcevich 1983 *Journal of Mathematical Analysis and Applications* **93**, 206–221. Application of differential quadrature to transport processes.
6. F. Civan and C. M. Sliepcevich 1983 *International Journal for Numerical Methods in Engineering* **19**, 711–724. Application of differential quadrature to transport processes.
7. J. R. Quan and C. T. Chang 1989 *Computers in Chemical Engineering* **13**, 779–788. New insights in solving distributed system equations by the quadrature methods—I. Analysis.
8. C. Shu and B. E. Richards 1992 *International Journal for Numerical Methods in Fluids* **15**, 791–798. Application of generalized differential quadrature to solve two-dimensional incompressible Navier–Stokes equations.
9. C. W. Bert, X. Wang and A. G. Striz 1993 *International Journal of Solids and Structures* **30**, 1737–1744. Differential quadrature for static and free vibration analysis of anisotropic plates.
10. C. W. Bert, X. Wang and A. G. Striz 1994 *Acta Mechanica* **102**, 11–24. Static and free vibrational analysis of beams and plates by differential quadrature method.
11. X. Wang and C. W. Bert 1993 *Journal of Sound and Vibration* **162**, 566–572. A new approach in applying differential quadrature to static and free vibrational analyses of beams and plates.

12. X. Wang, A. G. Striz and C. W. Bert 1993 *Journal of Sound and Vibration* **164**, 173–175. Free vibrational analysis of annular plates by the DQ method.
13. X. Wang, A. G. Striz and C. W. Bert 1994 *American Institute of Aeronautics and Astronautics Journal* **32**, 886–888. Buckling and vibrational analysis of skew plates by the differential quadrature method.
14. F.-L. Liu and K. M. Liew 1998 *Journal of Applied Mechanics* **65**(3), 705–710. Static analysis of Mindlin plates by differential quadrature element method.
15. F.-L. Liu and K. M. Liew 1998 *International Journal of Solids and Structures* **35**(28/29), 3655–3674. Differential cubature method for static solutions of arbitrarily shaped thick plates.
16. H. Du, K. M. Liew and M. K. Lim 1996 *Journal of Engineering Mechanics*, *ASCE* **122**, 95–100. Generalized differential quadrature method for buckling analysis.
17. P. A. A. Laura and R. H. Gutierrez 1993 *Shock and Vibration* **1**, 89–93. Analysis of vibrating Timoshenko beams using the method of differential quadrature.
18. C. Wen and Y. Yu 1993 *Computational Engineering* (B. M. Kwak and M. Tanaka, editors). Oxford: Elsevier Science, 163–168. Differential quadrature method for high order boundary value problems.
19. J.-B. Han and K. M. Liew 1995 *Proceedings of International Conference on Mechanics of Solids and Materials in Engineering* **B**, 580–585, 16–18 June, Singapore. Static response of Mindlin plates on Pasternak foundations: the generalised differential quadrature solution.
20. J.-B. Han and K. M. Liew 1996 *Proceedings of the Third Asian Pacific Conference on Computational Mechanics* **3**, 2363–2368. Seoul: Techno-Press. The differential quadrature element method (DQEM) for axisymmetric bending of thick circular plates.
21. K. M. Liew, J. B. Han, Z. M. Xiao and H. Du 1996 *International Journal of Mechanical Sciences* **38**(4), 405–421. Differential quadrature method for Mindlin plates on Winkler foundations.
22. K. M. Liew, J. B. Han and Z. M. Xiao 1996 *International Journal of Solids and Structures* **33**(18), 2647–2658. Differential quadrature method for thick symmetric cross-ply laminates with first-order shear flexibility.
23. K. M. Liew and J. B. Han 1997 *Journal of Engineering Mechanics*, *ASCE* **123**(3), 214–221. Bending analysis of simply supported shear deformable skew plates.
24. K. M. Liew and J. B. Han 1997 *Commun. Numerical Methods Eng.* **13**(2), 73–81. A four node differential quadrature method for straight-sided quadrilateral Reissner/Mindlin plates.
25. T. M. Teo and K. M. Liew 1997 *The 11th Asian Technical Exchange and Advisory Meeting on Marine Structures*, 129–136. Nanyang Technological University: Singapore. Free vibration of plate panels with three-dimensional flexibility.
26. T. M. Teo and K. M. Liew 1998 *International Journal of Solids and Structures* In press. A differential quadrature procedure for three-dimensional buckling analysis of rectangular plates.
27. K. M. Liew and T. M. Teo 1998 *Computer Methods in Applied Mechanics and Engineering* **159**(3–4), 369–381. Modeling via differential quadrature method: three-dimensional solutions for rectangular plates.
28. T. M. Teo 1998 *M. Eng. thesis. Nanyang Technological University*, *Singapore*. Three-dimensional analysis of plate panels based on differential quadrature method.
29. M. Malik and C. W. Bert 1998 *International Journal of Solids and Structures* **35**, 299–318. Three-dimensional elasticity Solutions for free vibrations of thick rectangular plates by the differential quadrature method.
30. S. Srinivas, C. V. Rao and A. K. Rao 1970 *Journal of Sound and Vibration* **12**, 187–199. An exact analysis for vibration of simply supported homogeneous and laminated thick rectangular plates.

31. S. Srinivas and A. K. Rao 1973 *Journal of Applied Mechanics* **40**, 298–299. Flexure of thick rectangular plates.
32. K. T. Iyengar, K. Chandrashekhara and V. K. Sebastian 1974 *Ingenieur Archiv* **43**, 317–339. On the analysis of thick rectangular plates.
33. J. R. Hutchinson and S. D. Zillimer 1983 *Journal of Applied Mechanics* **50**, 123–130. Vibration of a free rectangular parallelepiped.
34. A. W. Leissa and Z. D. Zhang 1983 *Journal of Acoustical Society of America* **73**, 2013–2021. On the three-dimensional vibrations of the cantilevered rectangular parallelepiped.
35. K. M. Liew, K. C. Hung and M. K. Lim 1993 *International Journal of Solids and Structures* **30**, 3357–3379. A continuum three-dimensional vibration analysis of thick rectangular plates.
36. K. M. Liew, K. C. Hung and M. K. Lim 1994 *International Journal of Solids and Structures* **31**, 3233–3247. Three-dimensional vibration of rectangular plates: variance of simple support conditions and influence of in-plane inertia.
37. K. M. Liew, K. C. Hung and M. K. Lim 1994 *Journal of Applied Mechanics* **61**, 159–165. Free vibration studies on stress-free three-dimensional elastic solids.
38. P. G. Young and S. M. Dickinson 1995 *Journal of Applied Mechanics* **62**, 706–708. Free vibration of a class of homogeneous isotropic solids.
39. C. W. Bert and M. Malik 1996 *Applied Mechanics Reviews* **49**, 1–28. Differential quadrature method in computational mechanics: a review.
40. A. W. Leissa 1973 *Journal of Sound and Vibration* **31**, 257–293. The free vibration of rectangular plates.
41. K. C. Hung 1996 *Ph. D. thesis. Nanyang Technological University, Singapore*. A treatise on three-dimensional vibration of a class of elastic solids.
42. D. J. Dawe 1985 in *Aspects of the Analysis of Plate Structures* (D. J. Dawe , R. W. Horsington, A. G. Kamtekar and G. H. Little, editors). Oxford: Clarendon Press, 73–99. Buckling and vibration of plate structures including shear deformation and related effects.
43. H. Matsunaga 1994 *International Journal of Solids and Structures* **31**, 3113–3124. Free vibration and stability of thick elastic plates subjected to inplane forces.
44. D. J. Gorman 1982 *Free Vibration Analysis of Rectangular Plates*. Elsevier North Holland: New York.
45. D. J. Dawe and O. L. Roufaeil 1980 *Journal of Sound and Vibration* **69**, 345–359. Rayleigh–Ritz vibration analysis of Mindlin plates.
46. K. M. Liew, Y. Xiang and S. Kitipornchai 1994 *Computers and Structures* **49**, 1–29. Transverse vibration of thick rectangular plates—I: comprehensive sets of boundary conditions (with shear correction factor $\kappa = 5/6$).
47. K. M. Liew, K. C. Hung and M. K. Lim 1995 *Journal of Sound and Vibration* **182**(1), 77–90. Vibration of Mindlin plates using boundary characteristics orthogonal polynomials.